



Article

Distributed Adaptive Formation Control for Fractional-Order Multi-Agent Systems with Actuator Failures and Switching Topologies

Jing Li * , Zixiang Yan, Xingyun Shi and Xuqiong Luo

School of Mathematics and Statistics, Changsha University of Science and Technology, Changsha 410114, China; yanzixiang2024@163.com (Z.Y.); sxy090402@163.com (X.S.); luoxuqiong@163.com (X.L.)

* Correspondence: lijingnew@126.com

Abstract: In this paper, a class of distributed adaptive formation control problems are investigated for second-order nonlinear fractional-order multi-agent systems with actuator failures and switching topologies. To address these challenges, two adaptive coupling gains based on agents' position and velocity are incorporated into the control protocol. Using the Lyapunov method along with graph theory and matrix analysis, sufficient conditions for system stability are derived in the presence of actuator failures and switching topologies. The effectiveness of the proposed control protocol is demonstrated through numerical simulations, which show its capability to maintain stable formation control under these challenging conditions.

Keywords: fractional-order multi-agent systems; adaptive formation control; Lyapunov method



Citation: Li, J.; Yan, Z.; Shi, X.; Luo, X. Distributed Adaptive Formation Control for Fractional-Order Multi-Agent Systems with Actuator Failures and Switching Topologies. *Fractal Fract.* **2024**, *8*, 563. <https://doi.org/10.3390/fractalfract8100563>

Academic Editor: António Lopes

Received: 8 August 2024

Revised: 21 September 2024

Accepted: 24 September 2024

Published: 28 September 2024



Copyright: © 2024 by the authors. Licensee MDPI, Basel, Switzerland. This article is an open access article distributed under the terms and conditions of the Creative Commons Attribution (CC BY) license (<https://creativecommons.org/licenses/by/4.0/>).

1. Introduction

In the past few decades, the rapid advancement of computing and network technologies has attracted widespread attention to distributed cooperative control in multi-agent systems. Its versatility and applicability make it a prevalent approach in systems science and control [1–7]. To address the varied needs of different tasks, cooperative control can be categorized into several types, including consensus, tracking, containment, and formation control [8–15], etc. The formation control is to achieve position and velocity control of all agents through information exchange, form specific geometries to complete complex cooperative tasks. Consequently, formation control for multi-agent systems is applied in various fields, including obstacle avoidance [16], multi-robot systems [17], and unmanned aerial vehicles [18], etc.

Recently, many scholars have explored formation control in multi-agent systems and achieved important research results. In [19], Liang et al. proposed a control strategy that uses relative local data and the desired formation structure to address the heterogeneous formation problem. In [20], Chen et al. addressed the problem of optimal control with uniformly moving leaders and developed a distributed control strategy with integrators for the followers. In [21], He et al. investigated formation control for linear multi-agent systems by using output feedback and an asynchronous sampled-data mechanism. These studies provide important research methods for the formation control of integer-order models. However, integer-order models have limitations in dealing with systems with memory effects and long time dependencies. As a result, there is increasing interest in using fractional-order models to achieve a more accurate representation of complex systems in formation control. In [22], Luo et al. used iterative control strategies and an initial learning rule for achieving finite-time formation control. In [23], Gong et al. introduced an observer-based distributed control approach and converted the time-varying formation control issues into a problem of asymptotic stability. In [24], Liu et al. explored formation control with relative damping and non-uniform symmetric delays, applying frequency domain

theory. In [25], Meng et al. introduced a dynamic event-triggered approach to address leader-follower formation control subject to external disturbances. In [26], Zamani et al. investigated fixed-time consensus and formation control under external disturbances by using the virtual structure method, and introduced a distributed sliding mode control approach based on neighborhood error variables.

Within multi-agent systems formation control, traditional methods typically rely on preset static parameters or fixed feedback gain matrices. These methods may perform poorly with dynamic changes or internal systems uncertainties. For example, dynamic changes between agents, sensor errors, or varying task requirements can affect the stability and performance of the formation. To overcome these challenges, adaptive techniques are introduced to enhance the robustness for multi-agent systems by real-time adjustment of control parameters. For instance, a time-varying parameter-adjustable adaptive control strategy was introduced to address the time-varying formation control problem [27]. In [28], Li et al. proposed a novel adaptive event-triggered control strategy aimed at reducing the constraints on control coefficients in the stability analysis of uncertain systems. In [29], Wang et al. explored the bounded Mittag-Leffler formation control issue, incorporating adaptive coupling gains into the triggering conditions and control protocols. In [30], Li et al. applied adaptive techniques to neural networks and employed a virtual leader approach to successfully achieve formation and obstacle avoidance for torpedo-type underactuated autonomous underwater vehicles.

It's worth noting that the studies mentioned above are based on a fixed topology, which often fails to account for the dynamic nature of real-world multi-agent systems where agents' positions and velocities continuously change. These variations frequently lead to switching topologies, which can adversely affect system performance by causing instability or loss of control inputs. To address these challenges, we focus on adaptive formation control for nonlinear fractional-order multi-agent systems. The adaptive control protocol is designed to dynamically adjust control inputs in response to these changes, including actuator failures, by continuously monitoring performance and recalibrating coupling gains. This adaptability ensures the stability of the formation and maintains resilience, allowing agents to achieve and sustain the desired configuration despite the loss of functionality in any single actuator.

- (1) Compared to the work in [24,26], we have developed a second-order nonlinear fractional-order multi-agent system model that incorporates both position and velocity information under actuator failure conditions and switching topologies. As a result, our research is more challenging, comprehensive, and practically relevant.
- (2) We generalise the multi-agent systems formation problem to fractional-order. The results presented in literature [31,32] primarily concern integer-order multi-agent systems, which can be regarded as a special case of this paper.
- (3) We propose a novel control protocol with two different adaptive coupling gains and establish a Lyapunov function involving actuator failures, error variables, and their derivatives. This provides new insights into formation control of fractional-order multi-agent systems under actuator failures and switching topologies.
- (4) This study enhances formation control by improving the robustness and adaptability of multi-agent systems in dynamic environments, which is crucial for applications such as unmanned aerial vehicles and robotic teams. It also develops fault-tolerant control strategies to maintain stability and performance during actuator failures and provides advanced control protocols for complex coordination tasks.

The remainder of the article is outlined as follows. In Section 2, we outline the necessary notations in Table 1, basic concepts of switching topologies, definitions and lemmas we will need later. In Section 3, we present the model and several assumptions necessary for the study. In Section 4, we outline the adaptive formation control strategy and conduct a stability analysis and theoretical proof. Finally, we demonstrate the correctness and superiority of the theoretical results through comparative experiments.

Table 1. Notations.

Symbol	Stand for
\mathbb{R}^n	n -dimensional Euclidean space
$\mathbb{R}^{n \times n}$	$n \times n$ real matrices
I_n	n -dimensional identity matrix
$\text{diag}(\dots)$	A diagonal matrix
$\ \cdot\ $ and \otimes	Vector 2-norm and Kronecker product
$P > 0$	Positive definite matrix P
$P < 0$	Negative definite matrix P
P^{-1}	Inverse of matrix P
P^T	Transpose of matrix P
$\lambda_{\max}(P)$	Maximal eigenvalue of matrix P
$\lambda_{\min}(P)$	Minimal eigenvalue of matrix P

2. Preliminaries

In the context of switching topology, the switching signal $\sigma(t)$ is defined on $[0, +\infty)$ and maps to the set $\{1, 2, \dots, s\}$, where s denotes the total number of possible topologies.

The communication network in multi-agent systems under switching topological structures is described by the undirected graph $G^{\sigma(t)} = (W, E^{\sigma(t)})$, where $W = \{w_1, w_2, \dots, w_N\}$ denotes the set of N followers in $G^{\sigma(t)}$, $E^{\sigma(t)} \subseteq W \times W$ stands for the edge set in $G^{\sigma(t)}$. $(w_i, w_j) \in E^{\sigma(t)}$ ($i, j = 1, 2, \dots, N$) denotes that nodes w_i and w_j are adjacent at time t . $A^{\sigma(t)} = [a_{ij}^{\sigma(t)}] \in \mathbb{R}^{N \times N}$ represents the adjacency matrix of $G^{\sigma(t)}$. If the i -th and j -th nodes are adjacent, then $a_{ij}^{\sigma(t)} = 1$; otherwise, $a_{ij}^{\sigma(t)} = 0$. Moreover, we assume that no node connects to itself, i.e., $a_{ii}^{\sigma(t)} = 0$ ($i = 1, 2, \dots, N$). The Laplacian matrix $L^{\sigma(t)} = [l_{ij}^{\sigma(t)}] \in \mathbb{R}^{N \times N}$ is defined with $l_{ii}^{\sigma(t)} = \sum_{j=1, j \neq i}^N a_{ij}^{\sigma(t)}$ and $l_{ij}^{\sigma(t)} = -a_{ij}^{\sigma(t)}$ for $i \neq j$.

Let $\bar{G}^{\sigma(t)}$ consist of one leader and N followers, $\mathcal{H}^{\sigma(t)} = L^{\sigma(t)} + B^{\sigma(t)}$ with $B^{\sigma(t)} = \text{diag}(b_1^{\sigma(t)}, b_2^{\sigma(t)}, \dots, b_N^{\sigma(t)})$. If the i -th follower communicates with the leader, $b_i^{\sigma(t)} = 1$; otherwise, $b_i^{\sigma(t)} = 0$.

Definition 1. ([33]). The fractional derivative of a function $f(t) \in C^n([0, \infty), \mathbb{R})$ in the Caputo sense is defined as

$$D^\alpha f(t) = \frac{1}{\Gamma(n - \alpha)} \int_0^t \frac{f^{(n)}(r)}{(t - r)^{\alpha + 1 - n}} dr,$$

where $\alpha \in (n - 1, n)$, $n \in \mathbb{Z}^+$, and $\Gamma(\cdot)$ represents the Gamma function.

Definition 2. ([33]). The one-parameter Mittag-Leffler functions is defined as

$$E_\alpha(z) = \sum_{k=1}^\infty \frac{z^k}{\Gamma(k\alpha + 1)},$$

where $z \in \mathbb{C}$, $\alpha > 0$.

Definition 3. Let $P \in \mathbb{R}^{m \times n}$ and $S \in \mathbb{R}^{p \times q}$. The Kronecker product $P \otimes S$ is a matrix in $\mathbb{R}^{mp \times nq}$, and is defined as

$$P \otimes S = \begin{pmatrix} p_{11}S & \cdots & p_{1n}S \\ \vdots & \ddots & \vdots \\ p_{m1}S & \cdots & p_{mn}S \end{pmatrix}.$$

It has the following properties

- (1) $P \otimes (S + K) = P \otimes S + P \otimes K;$
- (2) $(P \otimes S)^{-1} = P^{-1} \otimes S^{-1};$
- (3) $(P \otimes S)^T = P^T \otimes S^T;$
- (4) $(P \otimes S)(K \otimes M) = PK \otimes SM;$
- (5) $\iota(P \otimes S) = (\iota P) \otimes S = P \otimes (\iota S);$

where the matrices $P, S, K,$ and M are of appropriate dimensions, and ι is a scalar.

Definition 4. ([34]). If there exist constants $\hat{m} > 0, m > 0, \alpha \in (0, 1)$ and $\mu > 0,$ such that

$$\|e(t)\| \leq m(E_\alpha(-\hat{m}t^\alpha))^\mu, \quad t \geq 0,$$

then $e(t)$ is said to be Mittag-Leffler convergent to 0.

Lemma 1 ([35]). If the α -order derivative of a continuous function $V(t) : [0, +\infty) \rightarrow \mathbb{R}$ satisfying

$$D^\alpha V(t) \leq -\hat{m}V(t),$$

where $0 < \alpha < 1, \hat{m} > 0.$ Then

$$V(t) \leq V(0)E_\alpha(-\hat{m}t^\alpha), \quad t \geq 0.$$

Lemma 2. ([36]). Consider a differentiable vector function $y(t) : [0, \infty] \rightarrow \mathbb{R}^n,$ the following inequality holds

$$\frac{1}{2}D^\alpha \left(y^T(t) P y(t) \right) \leq y^T(t) P D^\alpha y(t),$$

where $\alpha \in (0, 1], P \in \mathbb{R}^{n \times n}$ is positive definite matrix.

Lemma 3. ([37]). For $\forall y \in \mathbb{R}^n,$ the following inequality holds:

$$\lambda_{\min} \left(C^{-1} Z \right) y^T C y \leq y^T Z y \leq \lambda_{\max} \left(C^{-1} Z \right) y^T C y,$$

where $C \in \mathbb{R}^{n \times n} > 0,$ and $Z \in \mathbb{R}^{n \times n}$ is a symmetric matrix.

Lemma 4. ([38]). For $\forall x \in \mathbb{R}^n, y \in \mathbb{R}^n$ and $Z > 0,$ the following inequality holds

$$2x^T y \leq x^T Z x + y^T Z^{-1} y,$$

Lemma 5. ([39]). The matrix $\mathcal{H}^{\sigma(t)} = L^{\sigma(t)} + B^{\sigma(t)}$ is positive definite if the leader can reach every node in $\overline{G}^{\sigma(t)}.$

3. Problem Formulation

In fractional-order multi-agent systems where there is one leader and N followers, the dynamics of the i -th follower is as follows

$$\begin{cases} D^\alpha \theta_i(t) = \varphi_i(t), \\ D^\alpha \varphi_i(t) = \delta_i^F(t) + \omega(t, \varphi_i(t)), \quad i = 1, 2, \dots, N. \end{cases} \quad (1)$$

The leader’s dynamic is given by

$$\begin{cases} D^\alpha \theta_0(t) = \varphi_0(t), \\ D^\alpha \varphi_0(t) = \omega(t, \varphi_0(t)), \end{cases} \tag{2}$$

where $0 < \alpha < 1$, $\theta_i(t) \in \mathbb{R}^n$, $\varphi_i(t) \in \mathbb{R}^n$ and $\delta_i^F(t) \in \mathbb{R}^n$ represent the position, velocity and control input of the i -th follower at time t , respectively. $\theta_0(t) \in \mathbb{R}^n$ and $\varphi_0(t) \in \mathbb{R}^n$ represent the position and velocity of the leader at time t . $\omega(t, \varphi_i(t)) \in \mathbb{R}^n$ and $\omega(t, \varphi_0(t)) \in \mathbb{R}^n$ are the inherent dynamics of followers and leader and satisfy the Lipschitz condition.

If a fault causes the actuator to respond inadequately to the control input signal, the effective control input $\delta_i^F(t)$ for the i -th follower is represented by

$$\delta_i^F(t) = (1 - \kappa_i(t))\delta_i(t), \quad i = 1, 2, \dots, N, \tag{3}$$

where $0 \leq \kappa_i(t) \leq \bar{\kappa} < 1$ is a time-dependent parameter that reflects the decrease in actuator efficiency for the i -th follower. When $\kappa_i(t) \equiv 0$, the actuator is fully operational; otherwise, it is functioning with reduced effectiveness. $\delta_i(t) \in \mathbb{R}^n$ represents the ideal control input assuming no faults. Based on the above description, we give the flowchart for the study of adaptive formation control for multi-agent systems in Figure 1.

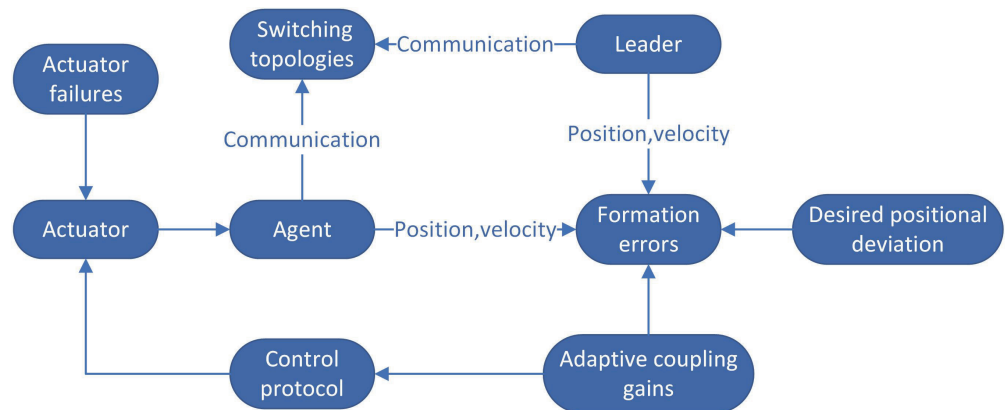


Figure 1. Flowchart for the study of adaptive formation control for multi-agent systems.

Remark 1. The functions $\omega(t, \varphi_i(t))$ and $\omega(t, \varphi_0(t))$ are key components of the system’s inherent dynamics, reflecting the intrinsic nonlinear characteristics of the system, which depend on time t and the velocities of the agents $\varphi_i(t)$ and $\varphi_0(t)$. Assume that these functions satisfy the Lipschitz condition, then the system’s response to changes in state variables is continuous and bounded, thereby guarantee the stability and robustness in the control design.

Assumption 1. $G^{\sigma(t)}$ is undirected and connected.

Assumption 2. $\bar{G}^{\sigma(t)}$ remains fixed and connected over the interval $[t_s, t_{s+1})$, where t_s denotes the moment of topology switch, and $t_0 = 0$.

Assumption 3. In $\bar{G}^{\sigma(t)}$, the leader can reach each node.

Assumption 4. For any $s_1, s_2 \in \mathbb{R}^n$, there exists a positive constant ρ such that

$$\| \omega(t, s_1) - \omega(t, s_2) \| \leq \rho \| s_1 - s_2 \| .$$

Definition 5. The systems (1) and (2) are considered to achieve the desired formation if the following conditions hold

$$\lim_{t \rightarrow +\infty} \| \theta_i(t) - \theta_0(t) - p_i \| = 0, \quad \lim_{t \rightarrow +\infty} \| \varphi_i(t) - \varphi_0(t) \| = 0, \quad i = 1, 2, \dots, N,$$

where $p_i \in \mathbb{R}^n$ represents the desired positional deviation of the i -th follower relative to the leader. The systems (1) and (2) are said to achieve consensus tracking if $p_i = 0$.

4. Main Results

In this section, we propose an adaptive control protocol to achieve formation control and analyze the stability of the systems and derive the sufficient conditions for achieving the desired formation.

Define variables $\bar{\theta}_i(t)$ and $\bar{\varphi}_i(t)$ for $i = 1, 2, \dots, N$ as

$$\begin{cases} \bar{\theta}_i(t) = \theta_i(t) - \theta_0(t) - p_i, \\ \bar{\varphi}_i(t) = \varphi_i(t) - \varphi_0(t). \end{cases} \quad (4)$$

Let $\bar{\theta}(t) = (\bar{\theta}_1^T(t), \bar{\theta}_2^T(t), \dots, \bar{\theta}_N^T(t))^T$, $\bar{\varphi}(t) = (\bar{\varphi}_1^T(t), \bar{\varphi}_2^T(t), \dots, \bar{\varphi}_N^T(t))^T$.

The distributed adaptive control protocol designed for the i -th follower is given as follows

$$\delta_i(t) = \delta_i^{\eta}(t) + \delta_i^{\xi}(t), \quad (5)$$

where

$$\begin{aligned} \delta_i^{\eta}(t) &= -\eta_i(t) \left[\sum_{j=1}^N a_{ij}^{\sigma(t)} (\theta_i(t) - p_i - \theta_j(t) + p_j) + b_i^{\sigma(t)} (\theta_i(t) - \theta_0(t) - p_i) \right] \\ &= -\eta_i(t) \left[\sum_{j=1}^N a_{ij}^{\sigma(t)} (\bar{\theta}_i(t) - \bar{\theta}_j(t)) + b_i^{\sigma(t)} \bar{\theta}_i(t) \right], \\ \delta_i^{\xi}(t) &= -\xi_i(t) \left[\sum_{j=1}^N a_{ij}^{\sigma(t)} (\varphi_i(t) - \varphi_j(t)) + b_i^{\sigma(t)} (\varphi_i(t) - \varphi_0(t)) \right] \\ &= -\xi_i(t) \left[\sum_{j=1}^N a_{ij}^{\sigma(t)} (\bar{\varphi}_i(t) - \bar{\varphi}_j(t)) + b_i^{\sigma(t)} \bar{\varphi}_i(t) \right], \end{aligned}$$

with $\eta_i(t)$, $\xi_i(t)$ ($i = 1, 2, \dots, N$) representing adaptive coupling gains of i -th agent, as defined in (8).

According to the Kronecker product, $\delta(t) = (\delta_1^T(t), \delta_2^T(t), \dots, \delta_N^T(t))^T$ can be expressed as

$$\delta(t) = - \left[(\eta(t) \mathcal{H}^{\sigma(t)}) \otimes I_n \right] \bar{\theta}(t) - \left[(\xi(t) \mathcal{H}^{\sigma(t)}) \otimes I_n \right] \bar{\varphi}(t), \quad (6)$$

where $\eta(t) = \text{diag}(\eta_1(t), \eta_2(t), \dots, \eta_N(t))$ and $\xi(t) = \text{diag}(\xi_1(t), \xi_2(t), \dots, \xi_N(t))$.

Let

$$\begin{aligned} \kappa(t) &= \text{diag}(\kappa_1(t), \kappa_2(t), \dots, \kappa_N(t)), \bar{\omega}(t, \varphi_i(t)) = \omega(t, \varphi_i(t)) - \omega(t, \varphi_0(t)), \\ \omega(t, \varphi(t)) &= (\bar{\omega}^T(t, \varphi_1(t)), \bar{\omega}^T(t, \varphi_2(t)), \dots, \bar{\omega}^T(t, \varphi_N(t)))^T. \end{aligned}$$

It follows that

$$\begin{cases} D^\alpha \bar{\theta}(t) = \bar{\varphi}(t), \\ D^\alpha \bar{\varphi}(t) = - \left\{ \left[(I_N - \kappa(t)) \eta(t) \mathcal{H}^{\sigma(t)} \right] \otimes I_n \right\} \bar{\theta}(t) \\ \quad - \left\{ \left[(I_N - \kappa(t)) \xi(t) \mathcal{H}^{\sigma(t)} \right] \otimes I_n \right\} \bar{\varphi}(t) + \omega(t, \varphi(t)). \end{cases} \quad (7)$$

We now present the following theorem to establish the effectiveness of the distributed control protocol (5).

Theorem 1. *If Assumptions 1–4 hold and the following conditions hold*

(i) The adaptive coupling gains $\eta_i(t)$ and $\xi_i(t)$ ($i = 1, 2, \dots, N$) are given by

$$\begin{cases} D^\alpha \eta_i(t) = a_i \left[\bar{\theta}^T(t) (\zeta_i \otimes I_n) \bar{\theta}(t) + \bar{\theta}^T(t) (\zeta_i \otimes I_n) \bar{\varphi}(t) \right], \\ D^\alpha \xi_i(t) = c_i \left[\bar{\varphi}^T(t) (\zeta_i \otimes I_n) \bar{\varphi}(t) + \bar{\theta}^T(t) (\zeta_i \otimes I_n) \bar{\varphi}(t) \right], \end{cases} \tag{8}$$

where a_i, c_i are positive constants, $\zeta_i = \left(h_{i1}^{\sigma(t)}, h_{i2}^{\sigma(t)}, \dots, h_{iN}^{\sigma(t)} \right)^T \left(h_{i1}^{\sigma(t)}, h_{i2}^{\sigma(t)}, \dots, h_{iN}^{\sigma(t)} \right)$.

(ii)

$$\begin{cases} (1 - \bar{\kappa}) \bar{\eta} \lambda_{\min}^2 \left(\mathcal{H}^{\sigma(t)} \right) - \frac{N \bar{h} (\rho + 1)}{2} > 0, \\ (1 - \bar{\kappa}) \bar{\xi} \lambda_{\min}^2 \left(\mathcal{H}^{\sigma(t)} \right) - \lambda_{\max} \left(\mathcal{H}^{\sigma(t)} \right) - \frac{N \bar{h} (3\rho + 1)}{2} > 0, \end{cases}$$

where $\bar{h} = \max_{1 \leq i, j \leq N} |h_{ij}^{\sigma(t)}|, \rho > 0, \bar{\eta}, \bar{\xi}$ are large enough constants. Then, under the distributed adaptive control protocol (5), the second-order fractional-order multi-agent systems (1) and (2) achieve formation control.

Proof of Theorem 1. Select a Lyapunov function

$$V(t) = V_1(t) + V_2(t), \tag{9}$$

where

$$\begin{aligned} V_1(t) &= \frac{1}{2} e^T(t) Q e(t), \quad e(t) = \left(\bar{\theta}^T(t), \bar{\varphi}^T(t) \right)^T, \\ V_2(t) &= \sum_{i=1}^N \frac{1 - \kappa_i(t)}{2a_i} (\eta_i(t) - \bar{\eta})^2 + \sum_{i=1}^N \frac{1 - \kappa_i(t)}{2c_i} (\xi_i(t) - \bar{\xi})^2, \\ Q &= \begin{pmatrix} \beta(t) \mathcal{H}^{\sigma(t)} \mathcal{H}^{\sigma(t)} + \mathcal{H}^{\sigma(t)} & \mathcal{H}^{\sigma(t)} \\ \mathcal{H}^{\sigma(t)} & \mathcal{H}^{\sigma(t)} \end{pmatrix} \otimes I_n, \\ \beta(t) &= \text{diag}(\beta_1(t), \beta_2(t), \dots, \beta_N(t)), \beta_i(t) > 0. \end{aligned}$$

Obviously, $V(t) \geq 0$.

According to (7) and Lemma 2, we have

$$\begin{aligned} D^\alpha V_1(t) &\leq e^T(t) Q D^\alpha e(t) \\ &= \bar{\theta}^T(t) \left[\left(\beta(t) \mathcal{H}^{\sigma(t)} \mathcal{H}^{\sigma(t)} + \mathcal{H}^{\sigma(t)} \right) \otimes I_n \right] \bar{\varphi}(t) + \bar{\varphi}^T(t) \left(\mathcal{H}^{\sigma(t)} \otimes I_n \right) \bar{\varphi}(t) \\ &\quad + \left(\bar{\theta}^T(t) + \bar{\varphi}^T(t) \right) \left(\mathcal{H}^{\sigma(t)} \otimes I_n \right) D^\alpha \bar{\varphi}(t) \\ &\leq \bar{\theta}^T(t) \left[\left(\beta(t) \mathcal{H}^{\sigma(t)} \mathcal{H}^{\sigma(t)} + \mathcal{H}^{\sigma(t)} \right) \otimes I_n \right] \bar{\varphi}(t) + \bar{\varphi}^T(t) \left(\mathcal{H}^{\sigma(t)} \otimes I_n \right) \bar{\varphi}(t) \\ &\quad - \bar{\theta}^T(t) \left\{ \left[\left(I_N - \kappa(t) \right) \mathcal{H}^{\sigma(t)} \eta(t) \mathcal{H}^{\sigma(t)} \right] \otimes I_n \right\} \bar{\theta}(t) \\ &\quad - \bar{\theta}^T(t) \left\{ \left[\left(I_N - \kappa(t) \right) \mathcal{H}^{\sigma(t)} \xi(t) \mathcal{H}^{\sigma(t)} \right] \otimes I_n \right\} \bar{\varphi}(t) \\ &\quad - \bar{\theta}^T(t) \left\{ \left[\left(I_N - \kappa(t) \right) \mathcal{H}^{\sigma(t)} \eta(t) \mathcal{H}^{\sigma(t)} \right] \otimes I_n \right\} \bar{\varphi}(t) \\ &\quad - \bar{\varphi}^T(t) \left\{ \left[\left(I_N - \kappa(t) \right) \mathcal{H}^{\sigma(t)} \xi(t) \mathcal{H}^{\sigma(t)} \right] \otimes I_n \right\} \bar{\varphi}(t) \\ &\quad + \left(\bar{\theta}^T(t) + \bar{\varphi}^T(t) \right) \left(\mathcal{H}^{\sigma(t)} \otimes I_n \right) \omega(t, \varphi(t)). \end{aligned} \tag{10}$$

Based on Assumption 4 and Lemma 4, we can get

$$\begin{aligned}
\bar{\theta}^T(t) \left(\mathcal{H}^{\sigma(t)} \otimes I_n \right) \omega(t, \varphi(t)) &= \sum_{i=1}^N \sum_{j=1}^N h_{ij}^{\sigma(t)} \bar{\theta}_i(t)^T (\omega(t, \varphi_j(t)) - \omega(t, \varphi_0(t))) \\
&\leq \sum_{i=1}^N \sum_{j=1}^N \rho \left| h_{ij}^{\sigma(t)} \right| \|\bar{\theta}_i(t)\| \|\bar{\varphi}_j(t)\| \\
&\leq \frac{N\bar{h}\rho}{2} \sum_{i=1}^N \left(\|\bar{\theta}_i(t)\|^2 + \|\bar{\varphi}_i(t)\|^2 \right),
\end{aligned} \tag{11}$$

where $\bar{h} = \max_{1 \leq i, j \leq N} |h_{ij}^{\sigma(t)}|$.
As above, we have

$$\begin{aligned}
\bar{\varphi}^T(t) \left(\mathcal{H}^{\sigma(t)} \otimes I_n \right) \omega(t, \varphi(t)) &= \sum_{i=1}^N \sum_{j=1}^N h_{ij}^{\sigma(t)} \bar{\varphi}_i(t)^T (\omega(t, \varphi_j(t)) - \omega(t, \varphi_0(t))) \\
&\leq \sum_{i=1}^N \sum_{j=1}^N \rho \left| h_{ij}^{\sigma(t)} \right| \|\bar{\varphi}_i(t)\| \|\bar{\varphi}_j(t)\| \\
&\leq N\bar{h}\rho \sum_{i=1}^N \|\bar{\varphi}_i(t)\|^2,
\end{aligned} \tag{12}$$

and

$$\begin{aligned}
\bar{\theta}^T(t) \left(\mathcal{H}^{\sigma(t)} \otimes I_n \right) \bar{\varphi}(t) &= \sum_{i=1}^N \sum_{j=1}^N h_{ij}^{\sigma(t)} \bar{\theta}_i^T(t) \bar{\varphi}_j(t) \\
&\leq \frac{N\bar{h}}{2} \sum_{i=1}^N \left(\|\bar{\theta}_i(t)\|^2 + \|\bar{\varphi}_i(t)\|^2 \right).
\end{aligned} \tag{13}$$

Then, we can obtain

$$\left(\bar{\theta}^T(t) + \bar{\varphi}^T(t) \right) \left(\mathcal{H}^{\sigma(t)} \otimes I_n \right) \omega(t, \varphi(t)) \leq \frac{N\bar{h}\rho}{2} \sum_{i=1}^N \|\bar{\theta}_i(t)\|^2 + \frac{3N\bar{h}\rho}{2} \sum_{i=1}^N \|\bar{\varphi}_i(t)\|^2. \tag{14}$$

Substituting (13) and (14) into (10), we can gain

$$\begin{aligned}
D^\alpha V_1(t) &\leq \bar{\theta}^T(t) \left[\left(\beta(t) \mathcal{H}^{\sigma(t)} \mathcal{H}^{\sigma(t)} \right) \otimes I_n \right] \bar{\varphi}(t) + \bar{\varphi}^T(t) \left(\mathcal{H}^{\sigma(t)} \otimes I_n \right) \bar{\varphi}(t) \\
&\quad - \bar{\theta}^T(t) \left\{ \left[(I_N - \kappa(t)) \mathcal{H}^{\sigma(t)} \eta(t) \mathcal{H}^{\sigma(t)} \right] \otimes I_n \right\} \bar{\theta}(t) \\
&\quad - \bar{\theta}^T(t) \left\{ \left[(I_N - \kappa(t)) \mathcal{H}^{\sigma(t)} \xi(t) \mathcal{H}^{\sigma(t)} \right] \otimes I_n \right\} \bar{\varphi}(t) \\
&\quad - \bar{\theta}^T(t) \left\{ \left[(I_N - \kappa(t)) \mathcal{H}^{\sigma(t)} \eta(t) \mathcal{H}^{\sigma(t)} \right] \otimes I_n \right\} \bar{\varphi}(t) \\
&\quad - \bar{\varphi}^T(t) \left\{ \left[(I_N - \kappa(t)) \mathcal{H}^{\sigma(t)} \xi(t) \mathcal{H}^{\sigma(t)} \right] \otimes I_n \right\} \bar{\varphi}(t) \\
&\quad + \frac{N\bar{h}(\rho+1)}{2} \sum_{i=1}^N \|\bar{\theta}_i(t)\|^2 + \frac{N\bar{h}(3\rho+1)}{2} \sum_{i=1}^N \|\bar{\varphi}_i(t)\|^2.
\end{aligned} \tag{15}$$

For $V_2(t)$, according to (8) and Lemma 2, one has

$$\begin{aligned}
 D^\alpha V_2(t) &\leq \sum_{i=1}^N \frac{1-\kappa_i(t)}{a_i} (\eta_i(t) - \bar{\eta}) D^\alpha \eta_i(t) + \sum_{i=1}^N \frac{1-\kappa_i(t)}{c_i} (\xi_i(t) - \bar{\xi}) D^\alpha \xi_i(t) \\
 &= \sum_{i=1}^N (1-\kappa_i(t)) (\eta_i(t) - \bar{\eta}) \left[\bar{\theta}^T(t) (\zeta_i \otimes I_n) \bar{\theta}(t) + \bar{\theta}^T(t) (\zeta_i \otimes I_n) \bar{\varphi}(t) \right] \\
 &\quad + \sum_{i=1}^N (1-\kappa_i(t)) (\xi_i(t) - \bar{\xi}) \left[\bar{\varphi}^T(t) (\zeta_i \otimes I_n) \bar{\varphi}(t) + \bar{\theta}^T(t) (\zeta_i \otimes I_n) \bar{\varphi}(t) \right] \\
 &= \bar{\theta}^T(t) \left\{ \left[(I_N - \kappa(t)) \mathcal{H}^{\sigma(t)} (\eta(t) - \Xi_1) \mathcal{H}^{\sigma(t)} \right] \otimes I_n \right\} \bar{\theta}(t) \\
 &\quad + \bar{\theta}^T(t) \left\{ \left[(I_N - \kappa(t)) \mathcal{H}^{\sigma(t)} (\eta(t) - \Xi_1) \mathcal{H}^{\sigma(t)} \right] \otimes I_n \right\} \bar{\varphi}(t) \\
 &\quad + \bar{\varphi}^T(t) \left\{ \left[(I_N - \kappa(t)) \mathcal{H}^{\sigma(t)} (\xi(t) - \Xi_2) \mathcal{H}^{\sigma(t)} \right] \otimes I_n \right\} \bar{\varphi}(t) \\
 &\quad + \bar{\theta}^T(t) \left\{ \left[(I_N - \kappa(t)) \mathcal{H}^{\sigma(t)} (\xi(t) - \Xi_2) \mathcal{H}^{\sigma(t)} \right] \otimes I_n \right\} \bar{\varphi}(t).
 \end{aligned} \tag{16}$$

where $\Xi_1 = \bar{\eta} I_N$, $\Xi_2 = \bar{\xi} I_N$.

Combining (15) with (16), it yields

$$\begin{aligned}
 D^\alpha V(t) &\leq \bar{\theta}^T(t) \left\{ \left[\beta(t) - (I_N - \kappa(t)) (\Xi_1 + \Xi_2) \right] \mathcal{H}^{\sigma(t)} \mathcal{H}^{\sigma(t)} \right\} \otimes I_n \bar{\varphi}(t) \\
 &\quad - (1 - \bar{\kappa}) \bar{\theta}^T(t) \left[\left(\mathcal{H}^{\sigma(t)} \Xi_1 \mathcal{H}^{\sigma(t)} \right) \otimes I_n \right] \bar{\theta}(t) \\
 &\quad + \bar{\varphi}^T(t) \left[\left(\mathcal{H}^{\sigma(t)} - (1 - \bar{\kappa}) \mathcal{H}^{\sigma(t)} \Xi_2 \mathcal{H}^{\sigma(t)} \right) \otimes I_n \right] \bar{\varphi}(t) \\
 &\quad + \frac{N\bar{h}(\rho+1)}{2} \sum_{i=1}^N \|\bar{\theta}_i(t)\|^2 + \frac{N\bar{h}(3\rho+1)}{2} \sum_{i=1}^N \|\bar{\varphi}_i(t)\|^2.
 \end{aligned} \tag{17}$$

Let $(1 - \kappa_i(t))\bar{\eta} = \eta_i^*(t)$, $(1 - \kappa_i(t))\bar{\xi} = \xi_i^*(t)$, $\beta_i(t) = \eta_i^*(t) + \xi_i^*(t)$, we can obtain $\beta(t) = (I_N - \kappa(t))(\Xi_1 + \Xi_2)$.

According to Lemma 3, we have

$$\begin{aligned}
 D^\alpha V(t) &\leq - \left((1 - \bar{\kappa}) \bar{\eta} \lambda_{\min}^2(\mathcal{H}^{\sigma(t)}) - \frac{N\bar{h}(\rho+1)}{2} \right) \bar{\theta}^T(t) \bar{\theta}(t) \\
 &\quad - \left((1 - \bar{\kappa}) \bar{\xi} \lambda_{\min}^2(\mathcal{H}^{\sigma(t)}) - \lambda_{\max}(\mathcal{H}^{\sigma(t)}) - \frac{N\bar{h}(3\rho+1)}{2} \right) \bar{\varphi}^T(t) \bar{\varphi}(t).
 \end{aligned} \tag{18}$$

Obviously, there exist sufficiently large $\bar{\eta}$, $\bar{\xi}$ such that

$$D^\alpha V(t) \leq 0. \tag{19}$$

Therefore, there exists $\hat{m} > 0$ such that

$$D^\alpha V(t) \leq -\hat{m}V(t). \tag{20}$$

According to Lemma 1, we can gain

$$V(t) \leq V(0)E_\alpha(-\hat{m}t^\alpha), \quad t \geq 0. \tag{21}$$

From (9), we have

$$\lambda_{\min}(Q)e(t)^T e(t) \leq 2V(t) \leq 2V(0)E_\alpha(-\hat{m}t^\alpha), \tag{22}$$

so

$$\|e(t)\| \leq m(E_\alpha(-\hat{m}t^\alpha))^{\frac{1}{2}}, \quad (23)$$

where $m = \sqrt{2V(0)\lambda_{\min}^{-1}(Q)}$.

Based on Definition 4, we can see $E_\alpha(-\hat{m}t^\alpha) \rightarrow 0$ as $t \rightarrow +\infty$, which leads to $V(t) = 0$, $e(t) = 0$. It implies that the systems (1) and (2) can achieve the Mittag-Leffler stability under designed control protocol (5). \square

5. Numerical Simulation

In this section, we conduct numerical simulations for the multi-agent system consisting of one leader and five followers. The proposed adaptive control protocol is compared against the traditional fixed-coupling gain control protocol. The switching topologies and the corresponding switching signal are illustrated in Figures 2 and 3. In these topologies, Node 0 represents the leader, while the remaining five nodes represent the followers. The edges between the nodes indicate the information exchange links. Specifically, when $\sigma(t) = 1$, the communication topology of the multi-agent system corresponds to \bar{G}^1 . Conversely, when $\sigma(t) = 2$, the communication topology switches to \bar{G}^2 . The computer configurations used for the simulations are provided in Tables 2 and 3.

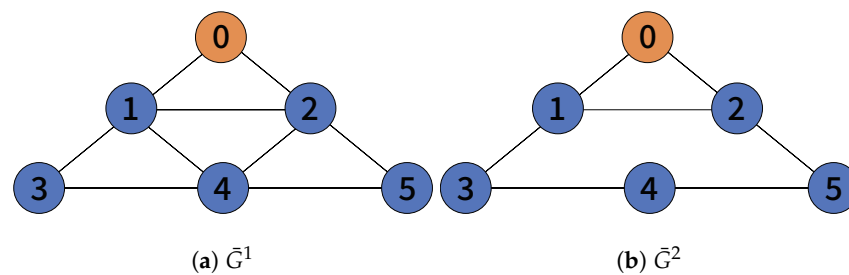


Figure 2. The switching topological structures.

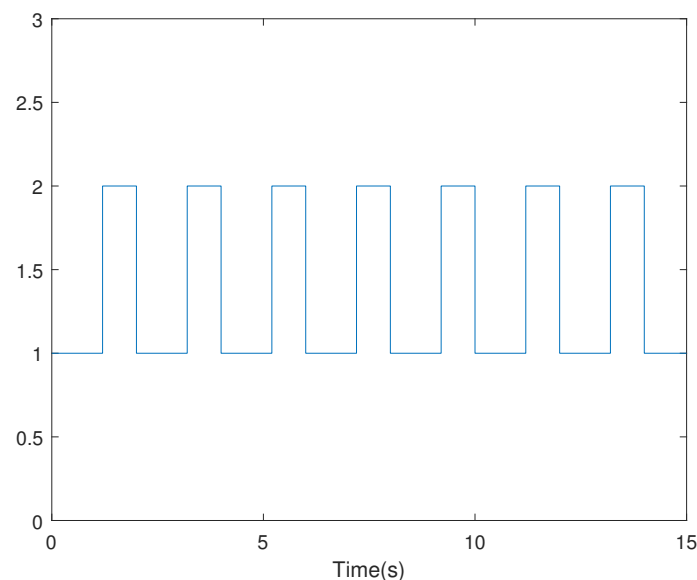


Figure 3. Switching signal.

Table 2. Computer Configurations.

Category	Specification
Processor	11th Gen Intel® Core™ i5-11500 @ 2.70 GHz
RAM	16.0 GB (15.7 GB available)
Storage	512 GB SSD
Graphics Card	NVIDIA GeForce GTX 1660 Super
Operating System	Windows 10 Professional

Table 3. Software Tools.

Simulation Tools	Application
MATLAB R2021b	Programming Language
Simulink/MATLAB R2021b	For performing optimization tasks
FOTF Toolbox	Provide key simulation modules

Based on Figure 2, the matrices \mathcal{H}^1 and \mathcal{H}^2 for the switching topologies can be derived as follows

$$H^1 = \begin{pmatrix} 4 & -1 & -1 & -1 & 0 \\ -1 & 4 & 0 & -1 & -1 \\ -1 & 0 & 2 & -1 & 0 \\ -1 & -1 & -1 & 4 & -1 \\ 0 & -1 & 0 & -1 & 2 \end{pmatrix}, \quad H^2 = \begin{pmatrix} 3 & -1 & -1 & 0 & 0 \\ -1 & 3 & 0 & 0 & -1 \\ -1 & 0 & 2 & -1 & 0 \\ 0 & 0 & -1 & 2 & -1 \\ 0 & -1 & 0 & -1 & 2 \end{pmatrix}.$$

Next, the nonlinear terms for each agent $i = 0, 1, 2, 3, 4, 5$ are defined as

$$\omega(t, \varphi_i(t)) = \begin{pmatrix} \sin \varphi_{i1}(t) \\ e^{-0.01\varphi_{i2}(t)} \\ \sin \varphi_{i3}(t) \end{pmatrix}.$$

Based on these settings, we obtain $\rho = 1$, $\lambda_{\max}(\mathcal{H}^{\sigma(t)}) = 5.3028$ and $\lambda_{\min}(\mathcal{H}^{\sigma(t)}) = 0.2679$.

To simulate actuator failures, we define the loss of actuator effectiveness $\kappa_i(t)$ for each follower $i = 1, 2, \dots, 5$ as follows

$$\kappa_1(t) = \begin{cases} 0, & 0 \leq t < 4, \\ 0.3, & t \geq 4, \end{cases} \quad \kappa_2(t) = \begin{cases} 0, & 0 \leq t < 3, \\ 0.2, & t \geq 3, \end{cases}$$

$$\kappa_3(t) = \begin{cases} \frac{1}{1+e^t}, & 0 \leq t < 5, \\ \frac{1}{1+e^5}, & t \geq 5, \end{cases} \quad \kappa_4(t) = 0.25, \quad \kappa_5(t) = 0.1.$$

The average actuator loss is $\bar{\kappa} = 0.3$.

Let $\alpha = 0.97$. For the adaptive coupling gains defined in (8), we set the parameters as follows

$$a_i = c_i = 1, \quad i = 1, 2, \dots, 5.$$

The initial values are given by

$$\eta_i(0) = \xi_i(0) = 0.1 \cdot i, \quad i = 1, 2, \dots, 5.$$

The initial positions of the leader and followers are randomly generated and specified as

$$\begin{aligned} \theta_0(0) &= (-7.9, -2.1, 7.6)^T, & \theta_1(0) &= (-0.1, 5.5, 4.3)^T, \\ \theta_2(0) &= (-8, -7.8, 1)^T, & \theta_3(0) &= (4, -6, 2.4)^T, \\ \theta_4(0) &= (3.7, 4.1, 6.3)^T, & \theta_5(0) &= (-10, 5, 3)^T. \end{aligned}$$

The initial velocities for the leader and followers are

$$\varphi_0(0) = (0.2, 0.2, 0.2)^T, \quad \varphi_i(0) = (0.1, 0.1, 0.1)^T \quad (i = 1, 2, \dots, 5).$$

Finally, the desired formation geometry is defined as

$$p_1 = (6, 0, 0)^T, \quad p_2 = (9, -\sqrt{3}, 3)^T, \quad p_3 = (6, -6\sqrt{3}, 6)^T, \\ p_4 = (0, -6\sqrt{3}, 6)^T, \quad p_5 = (-3, -3\sqrt{3}, 3)^T.$$

Figure 4 shows snapshots of the leader and followers' positions at different time in three-dimensional space, applying the adaptive control protocol (5). By connecting the agents in these snapshots, it is evident that all agents gradually form and maintain a regular hexagon configuration, indicating successful coordination and stability within the multi-agent system. This formation serves as a strong testament to the efficacy of the proposed control protocol (5). Figure 5 depicts the trajectory of the adaptive coupling gains, which ultimately converge to a constant value. This shows that the adaptive gains stabilize after a period of adjustment, reinforcing the reliability and robustness of the control approach.

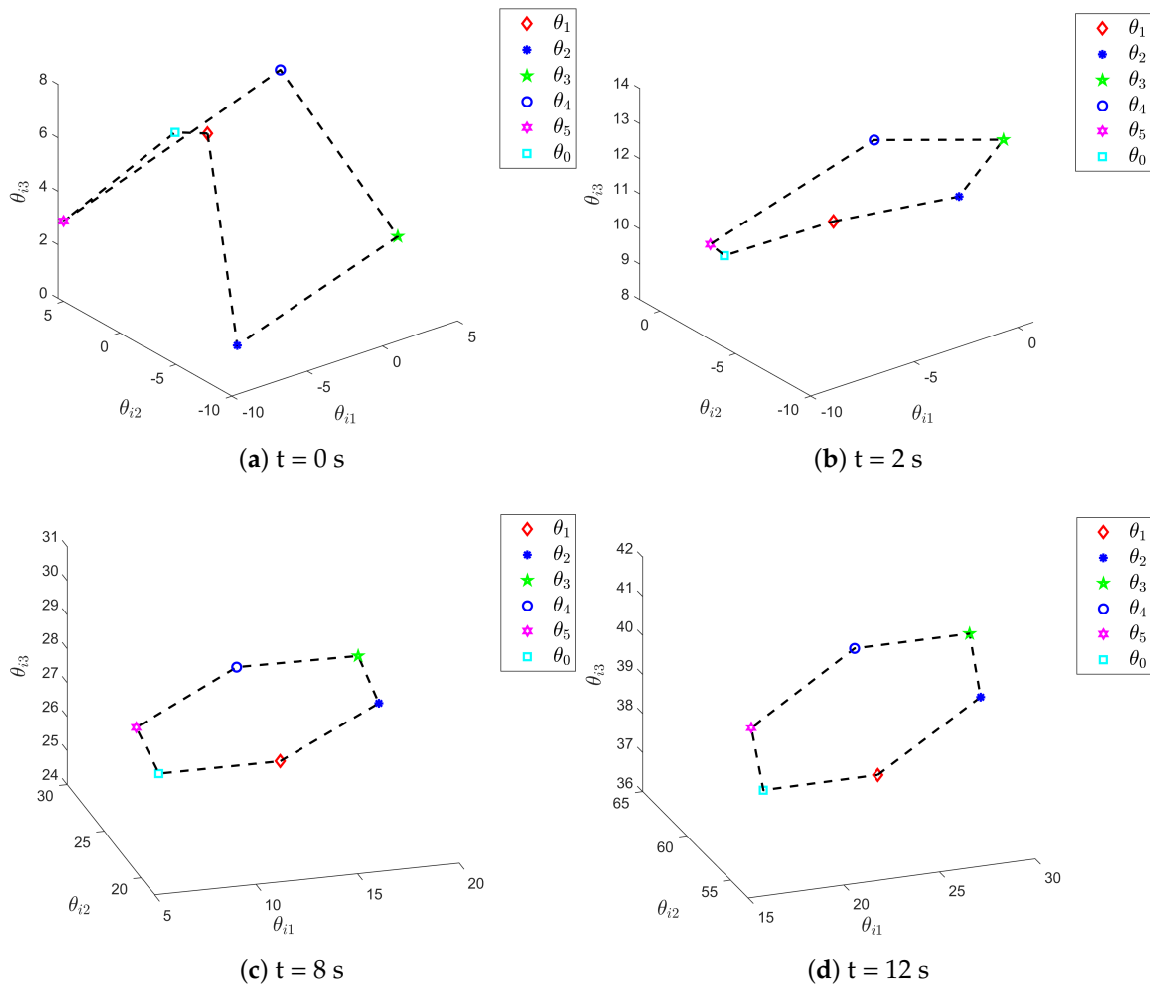


Figure 4. Position snapshots at different times for each agent.

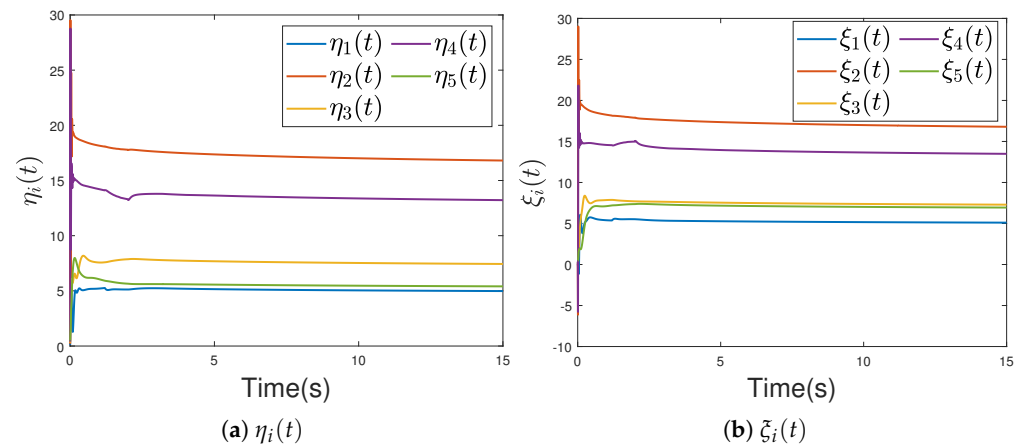


Figure 5. Adaptive coupling gains.

Figures 6 and 7 illustrate the variations of the position and the velocity trajectories, respectively. In these figures, the solid lines represent the motion trajectories achieved under adaptive coupling gain control, while the dashed lines correspond to those under fixed coupling gain control. It is worth noting that while both methods lead to a gradual convergence of position and velocity errors to zero, our approach exhibits a significantly faster convergence rate compared to traditional methods. This observation highlights the effectiveness of the adaptive control strategy in enhancing performance.

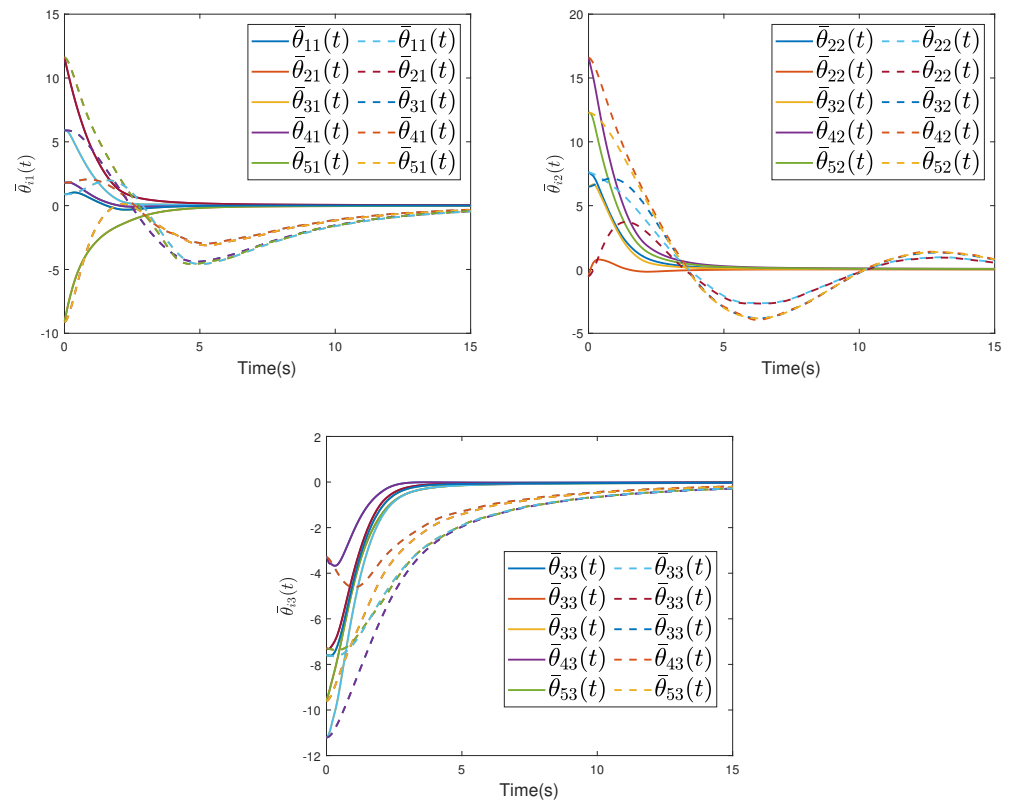


Figure 6. Position errors $\bar{\theta}_{i1}(t)$, $\bar{\theta}_{i2}(t)$ and $\bar{\theta}_{i3}(t)$.

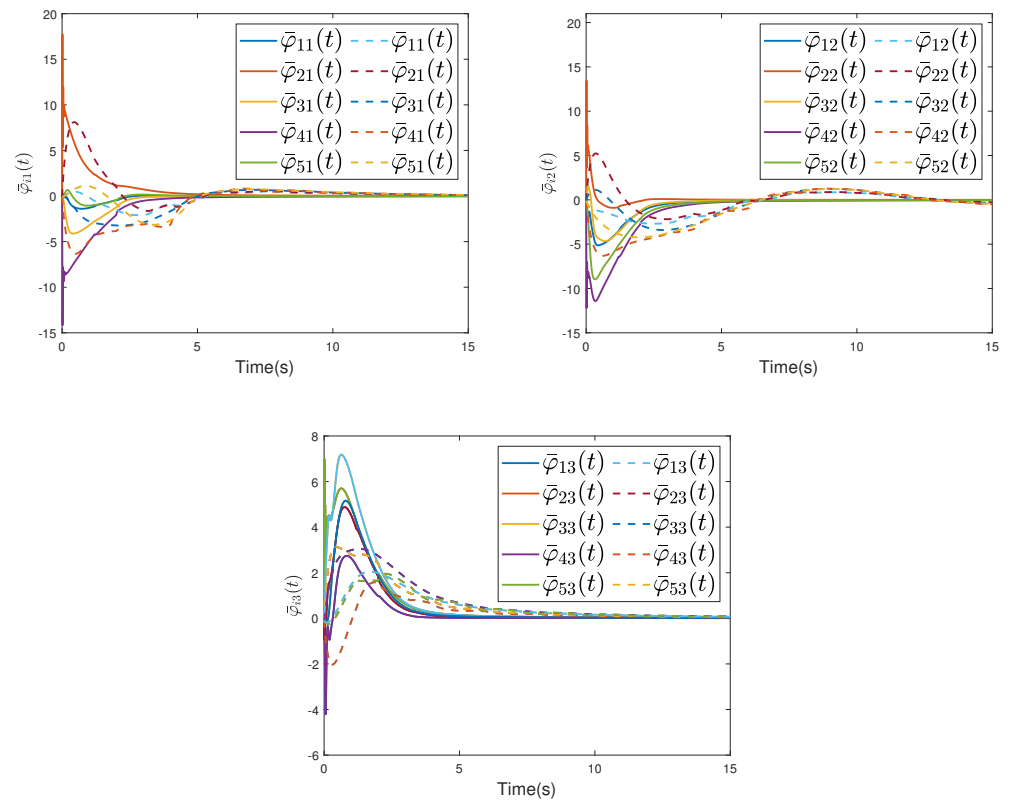


Figure 7. Speed errors $\bar{\varphi}_{i1}(t)$ a, $\bar{\varphi}_{i2}(t)$ and $\bar{\varphi}_{i3}(t)$.

Finally, Figure 8 presents the trajectory of the control inputs over time, providing insights into the dynamics of the control mechanism employed. Overall, these results collectively demonstrate the effectiveness and potential of the proposed control strategy in achieving desired formation and stability in fractional-order multi-agent systems.

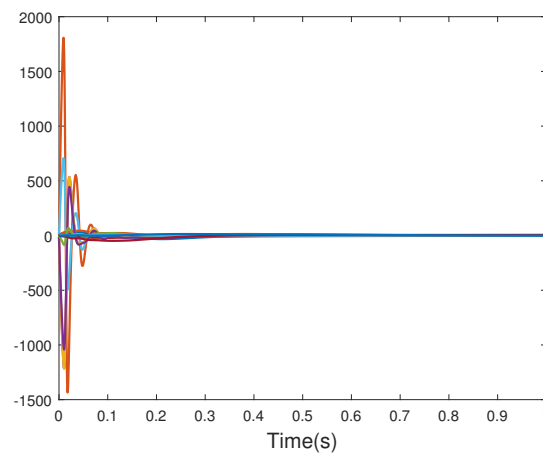


Figure 8. Control input.

6. Conclusions

In this paper, we put forward a novel distributed adaptive formation control protocol for second-order nonlinear fractional-order multi-agent systems that are subject to the effects of actuator failures and switching topologies. The incorporation of adaptive coupling gains markedly enhanced the resilience of the system to dynamic disturbances. The correctness of the theoretical results is further illustrated by implementing a formation control task for a positive hexagon. These results not only extend the theoretical understanding

of fractional-order systems, but also provide practical insights for the design of resilient multi-agent networks. Notwithstanding the success of the proposed approach, certain limitations remain. For instance, the present model is based on the assumption of ideal communication between agents, which may not be applicable in real-world scenarios that involve delays or noise. Furthermore, the scalability of the method to larger networks requires further investigation. In future, we will concentrate on resolving communication delays, addressing external disturbances and applying the proposed control framework to more complex multi-agent systems.

Author Contributions: Conceptualization, J.L., Z.Y. and X.S.; methodology, J.L., Z.Y. and X.S.; software, Z.Y. and X.S.; validation, J.L., Z.Y. and X.L.; formal analysis, J.L., Z.Y., X.S. and X.L.; investigation, J.L. and X.S.; writing—original draft preparation, Z.Y.; writing—review and editing, J.L.; visualization, X.L. and X.S.; supervision, J.L.; funding acquisition, J.L. All authors have read and agreed to the published version of the manuscript.

Funding: The first author was supported by the National Natural Science Foundation of China grant (12126408), Hunan Provincial Natural Science Foundation of China grant (2024JJ5004).

Data Availability Statement: Data are contained within the article.

Conflicts of Interest: The authors declare no conflict of interest.

References

1. Rezaee, H.; Abdollahi, F. A decentralized cooperative control scheme with obstacle avoidance for a team of mobile robots. *IEEE Trans. Ind. Electron.* **2024**, *61*, 347–354. [[CrossRef](#)]
2. Li, Z.; Chen, J. Robust consensus of linear feedback protocols over uncertain network graphs. *IEEE Trans. Autom. Control* **2017**, *62*, 4251–4258. [[CrossRef](#)]
3. Zhao, S. Affine formation maneuver control of multiagent systems. *IEEE Trans. Autom. Control.* **2018**, *63*, 4140–4155. [[CrossRef](#)]
4. Luo, D.; Wang, J.; Shen, D. PD^α -type distributed learning control for nonlinear fractional-order multiagent systems. *Math. Methods Appl. Sci.* **2019**, *42*, 4543–4553. [[CrossRef](#)]
5. Donganont, M.; Liu, X. Scaled consensus problems of multi agent systems via impulsive protocols. *Appl. Math. Model.* **2023**, *116*, 532–546. [[CrossRef](#)]
6. Thanh, H.L.N.N.; Vu, M.T.; Mung, N.X.; Nguyen, N.P.; Phuong, N.T. Perturbation observer-based robust control using a multiple sliding surfaces for nonlinear systems with influences of matched and unmatched uncertainties. *Mathematics* **2020**, *8*, 1371. [[CrossRef](#)]
7. Alattas, K.A.; Mohammadzadeh, A.; Mobayen, S.; Abo-Dief, H.M.; Alanazi, A.K.; Vu, M.T.; Chang, A. Automatic control for time delay markov jump systems under polytopic uncertainties. *Mathematics* **2022**, *10*, 187. [[CrossRef](#)]
8. Fan, Y.; Jin, Z.; Luo, X.; Guo, B. Robust finite-time consensus control for euler-lagrange multi-agent systems subject to switching topologies and uncertainties. *Appl. Math. Comput.* **2022**, *432*, 127367. [[CrossRef](#)]
9. Qin, Z.; Wu, H.; Wang, J. Proactive cooperative consensus control for a class of human-in-the-loop multi-agent systems with human time-delays. *Neurocomputing* **2024**, *581*, 127485. [[CrossRef](#)]
10. Cui, B.; Wang, Y.; Liu, K.; Xia, Y. Sliding mode based prescribed-time consensus tracking control of second-order multi-agent systems. *Automatica* **2023**, *158*, 111296. [[CrossRef](#)]
11. Liang, M.; Li, J. Distributed data-driven iterative learning point-to-point consensus tracking control for unknown nonlinear multi-agent systems. *Neurocomputing* **2023**, *561*, 126875. [[CrossRef](#)]
12. Liu, S.; Fu, X.; Zhao, X.; Pang, D. Containment control for fractional-order multi-agent systems with mixed time delays. *Mathematical Methods in the Appl. Sci.* **2023**, *46*, 3176–3186. [[CrossRef](#)]
13. Sun, H.; Xia, R.; Yu, A. Fully distributed containment control for second-order nonlinear multi-agent systems with external disturbances. *IEEE Trans. Circuits Syst. II Express Briefs* **2022**, *69*, 2126–2130. [[CrossRef](#)]
14. Gao, Z.; Guo, G. Velocity free leader-follower formation control for autonomous underwater vehicles with line-of-sight range and angle constraints. *Inf. Sci.* **2019**, *486*, 359–378. [[CrossRef](#)]
15. Wang, J.; Dong, H.; Chen, F.; Vu, M.T.; Shakibjoo, A.D.; Mohammadzadeh, A. Formation control of non-holonomic mobile robots: Predictive data-driven fuzzy compensator. *Mathematics* **2023**, *11*, 1804. [[CrossRef](#)]
16. Wen, G.; Chen, C.L.P.; Liu, Y. Formation control with obstacle avoidance for a class of stochastic multiagent systems. *IEEE Trans. Ind. Electron.* **2018**, *65*, 5847–5855. [[CrossRef](#)]
17. Wang, C.; Ji, J.; Miao, Z.; Zhou, J. Formation tracking of multi-robot systems with switching directed topologies based on udwadia-kalaba approach. *Appl. Math. Model.* **2024**, *126*, 147–158. [[CrossRef](#)]
18. Li, Q.; Chen, Y.; Liang, K. Predefined-time formation control of the quadrotor-uav cluster' position system. *Appl. Math. Model.* **2023**, *116*, 45–64. [[CrossRef](#)]

19. Liang, S.; Wang, F.; Chen, Z.; Liu, Z. Formation control for discrete-time heterogeneous multi-agent systems. *Int. J. Robust Nonlinear Control* **2022**, *32*, 5848–5865. [[CrossRef](#)]
20. Chen, S.; Dai, J.; Yi, J.; Chai, L. An optimal design of the leader-following formation control for discrete multi-agent systems. *IFAC-PapersOnLine* **2022**, *55*, 201–206. [[CrossRef](#)]
21. He, Q.; Liu, W. Formation control for linear multi-agent systems with asynchronously sampled outputs. *Inf. Sci.* **2024**, *658*, 119992. [[CrossRef](#)]
22. Luo, D.; Wang, J.; Shen, D. Learning formation control for fractional-order multiagent systems. *Math. Methods Appl. Sci.* **2018**, *41*, 5003–5014. [[CrossRef](#)]
23. Gong, Y.; Wen, G.; Peng, Z.; Huang, T.; Chen, Y. Observer-based time-varying formation control of fractional-order multi-agent systems with general linear dynamics. *IEEE Trans. Circuits Syst. II Express Briefs* **2019**, *67*, 82–86. [[CrossRef](#)]
24. Liu, J.; Li, P.; Chen, W.; Qin, K.; Qi, L. Distributed formation control of fractional-order multi-agent systems with relative damping and nonuniform time-delays. *Isa Trans.* **2019**, *93*, 189–198. [[CrossRef](#)] [[PubMed](#)]
25. Meng, X.; Jiang, B.; Karimi, H.R.; Gao, C. Leader–follower sliding mode formation control of fractional-order multi-agent systems: A dynamic event-triggered mechanism. *Neurocomputing* **2023**, *557*, 126691. [[CrossRef](#)]
26. Zamani, H.; Khandani, K.; Majd, V.J. Fixed-time sliding-mode distributed consensus and formation control of disturbed fractional-order multi-agent systems. *Isa Trans.* **2023**, *138*, 37–48. [[CrossRef](#)]
27. Deng, J.; Li, K.; Wu, S.; Wen, Y. Distributed adaptive time-varying formation tracking control for general linear multi-agent systems based on event-triggered strategy. *IEEE Access* **2020**, *8*, 13204–13217. [[CrossRef](#)]
28. Li, Y.; Hu, X.; Che, W.; Hou, Z. Event-based adaptive fuzzy asymptotic tracking control of uncertain nonlinear systems. *IEEE Trans. Fuzzy Syst.* **2020**, *29*, 3003–3013. [[CrossRef](#)]
29. Wang, Y.; Zhang, J.; Wu, H. Distributed adaptive mittag–leffler formation control for second-order fractional multi-agent systems via event-triggered control strategy. *Fractal Fract.* **2022**, *6*, 380. [[CrossRef](#)]
30. Li, J.-H.; Kang, H.; Kim, M.-G.; Lee, M.-J.; Cho, G.R.; Jin, H.-S. Adaptive formation control of multiple underactuated autonomous underwater vehicles. *J. Mar. Sci. Eng.* **2022**, *10*, 1233. [[CrossRef](#)]
31. Wang, M.; Zhang, T. Leader-following formation control of second-order nonlinear systems with time-varying communication delay. *Int. J. Control. Autom. Syst.* **2021**, *19*, 1729–1739. [[CrossRef](#)]
32. Xiong, T.; Gu, Z. Observer-based adaptive fixed-time formation control for multi-agent systems with unknown uncertainties. *Neurocomputing* **2021**, *423*, 506–517. [[CrossRef](#)]
33. Podlubny, I. *Fractional Differential Equations*; Academic Press: San Diego, CA, USA, 1999.
34. Peng, X.; Wu, H.; Song, K.; Shi, J. Global synchronization in finite time for fractional-order neural networks with discontinuous activations and time delays. *Neural Netw.* **2017**, *94*, 46–54. [[CrossRef](#)] [[PubMed](#)]
35. Gong, P. Distributed tracking of heterogeneous nonlinear fractional-order multi-agent systems with an unknown leader. *J. Frankl. Inst.* **2017**, *354*, 2226–2244. [[CrossRef](#)]
36. Duarte-Mermoud, M.A.; Aguila-Camacho, N.; Gallegos, J.A.; Castro-Linares, R. Using general quadratic lyapunov functions to prove lyapunov uniform stability for fractional order systems. *Commun. Nonlinear Sci. Numer. Simul.* **2015**, *22*, 650–659. [[CrossRef](#)]
37. Huang, L. *Linear Algebra in System and Control Theory*; Science Press: Beijing, China, 1984.
38. Wu, M.; He, Y.; She, J. *Stability Analysis and Robust Control of Time-Delay Systems*; Springer: Berlin/Heidelberg, Germany, 2010.
39. Hu, J.; Hong, Y. Leader-following coordination of multi-agent systems with coupling time delays. *Phys. A Stat. Mech. Its Appl.* **2007**, *374*, 853–863. [[CrossRef](#)]

Disclaimer/Publisher’s Note: The statements, opinions and data contained in all publications are solely those of the individual author(s) and contributor(s) and not of MDPI and/or the editor(s). MDPI and/or the editor(s) disclaim responsibility for any injury to people or property resulting from any ideas, methods, instructions or products referred to in the content.